PCCP

Accepted Manuscript

ROYAL SOCIETY OF CHEMISTRY

www.rsc.org/pccp

Journal Name

RSCPublishing

ARTICLE

Optical manipulation of single molecules in the living cell

ite this: DOI: 10.1039/x0xx00000x

Kamilla Norregaard,[a] Liselotte Jauffred,[a] Kirstine Berg-Sørensen[b] and Lene B. Oddershede[a] ,

Received 15th January 2014,
Accepted ooth January 2014

DOI: 10.1039/x0xx00000x

www.rsc.org/

Optical tweezers are the only nano-tool capable of manipulating and performing force-measurements on individual molecules and organelles within the living cell without performing a destructive penetration through the cell wall and without the need of inserting a non-endogenous probe. Here, we describe how optical tweezers are used to manipulate individual molecules and perform accurate force and distance measurements within the complex cytoplasm of the living cell. Optical tweezers can grab individual molecules or organelles, if their optical contrast to the medium is large enough, as is the case, e.g., for lipid granules or chromosomes. However, often the molecule of interest is specifically attached to a handle manipulated by the optical trap. The most commonly used handles, their insertion into the cytoplasm, and the relevant micro-rheology of the cell are here discussed and we also review recent and exciting results achieved through optical force manipulation of individual molecules *in vivo*.

Introduction

Since the invention of optical trapping[1] and the discovery that living microorganisms could survive being optically trapped for long periods of time,[2] optical traps have had great success uncovering fundamentals of biological systems at the single molecule level.[3, 4] One reason for this success is probably that optical traps are capable of measuring forces and distances in the pico-Newton and nanometer range, which are exactly the forces and distances of interest at the single molecule level of the cellular machinery. Another reason which is particularly important with respect to *in vivo* single molecule measurements is that optical trapping, even inside a living cell, can be performed almost non-invasively,[5] which is in contrast to, e.g., atomic force measurements where the cantilever would need to physically penetrate the cell membrane in order to perform measurements inside a cell. Magnetic tweezers can also operate non-invasively inside living cells, but a magnetic probe particle would need to be inserted into the cytoplasm.

Optical traps belong to the toolbox of techniques capable of observing individual molecules for an extended period of time. Single molecule studies can reveal rare and transient events or dynamical behaviour of single molecules, thus unravelling fundamental properties of bio-molecules that are typically hidden in ensemble studies. In addition to simple video based tracking of individual molecules, which can also be performed with high accuracy, e.g., by the novel super-resolution techniques,[6, 7] optical traps are capable of exerting and measuring forces. Force has an important role driving the fundamental processes of the living cell. For instance, force is known to guide cell motility,[8] be important for cell-environment communication, influence stem cell differentiation[9], and of course be important for intra-cellular cargo transportation by molecular motors and cytoskeletal re-organization, also during the division.

Most biomolecules are controlled in a hierarchical manner by their local environment through signalling pathways, topological constraints, and mechanical forces that all can modulate the biomolecule's function. *In vitro* optical tweezers measurements have successfully uncovered mechanical and dynamic properties of many molecular motors. For example the run length, step-size, velocity, and load dependence of cytoskeletal motor molecules such as kinesin[10-12] and myosin.[13, 14] Also, optical tweezers have been extremely useful in characterizing the mechanical properties of bio-polymers such as DNA, microtubules[15] or actin,[16] pinpointing, e.g., DNA's force-extension relation,[17, 18] melting,[19, 20] and twisting[18] properties as well as its interaction with various proteins.[19, 21] *In vitro* single molecule investigations have the distinct advantage of being able to investigate the influence of one well defined parameter at a time, which is important, e.g., for quantifying the coupling between mechanical work and a molecular motor's energy consumption.[11]

In vitro studies have laid the foundation for our understanding of force-dependent and dynamical events of biomolecules. However, purifying and removing a single biomolecule from its natural environment may alter its properties and render *in vitro* results less biologically relevant than observations done within the living cell. Dynein is an example of a molecular motor where *in vivo* observations indicate that the motor is less processive inside a living cell[22] than in a test tube.[23] However the interpretation of such results

is not trivial as dynein cannot depart from its cargo as easily in vivo as in vitro and the number of motors attached to the cargo is not easily determined in vivo. Also ribosomes are reported to translate significantly slower *in vitro* than *in vivo*.[5]

Despite the great interest and development of single molecule techniques capable of reaching inside the living cell[5] the results obtained *in vivo* are still limited. This is probably due to the severe challenges associated with bringing single molecule force-measuring techniques into the living cell.[5, 24] Here, we focus on optical force manipulation inside living cells, explain how to overcome the *in vivo* challenges, and lay out the methodology for *in vivo* force calibration and measurements. Also we discuss the important issues of internalizing the handle for the optical trap into the living cell and the micro-rheological properties of the cytoplasm. Finally, we review exciting results recently obtained through optical manipulation of single molecules *in vivo*.

Experimental

Optical tweezers are typically formed by tightly focusing a laser beam to a diffraction-limited spot using a high numerical aperture (NA) objective. Figure 1 shows a setup where an optical trap (the infrared light originating from a 1064 nm Nd:YVO_4 laser) is implemented in a confocal microscope. This type of setup allows for simultaneous force measurements and confocal visualization of fluorescently marked molecules and handles. Equipped with appropriate detection schemes, as for instance photodiodes in the back-focal plane, optical tweezers can measure displacements in three dimensions with a spatial resolution down to 0.2 nm and a temporal resolution on the order of μs. Often the beam profile of the trapping laser is Gaussian because it provides a small well defined focal spot and produces a large optical gradient, hence, a large force. The trapped object experiences a force, F, that is a combination of gradient and scattering forces. The equilibrium position is normally close to the focus of the laser beam, however, it could be displaced somewhat in the axial direction because of the scattering force.[25] For small displacements of the trapped object the force scales linearly with displacement, x. In this regime, the optical trap is well-described as a Hookian spring, $F = -\kappa x$, where κ is denoted the spring constant. κ has a different value in each of the translational directions, is typically weaker in the axial direction than in the lateral directions, and normally has a value of ~0.01-1 pN nm^{-1}, depending on laser power and alignment.

For biological applications, optical tweezers based on near-infrared lasers (850-1064 nm) are preferable because biological tissue and water absorbs only very little light at those wavelengths. To create a strong trap based on a single laser beam it is advantageous to use a high NA objective. Oil immersion objective are available with higher NA than water immersion objectives, however, an oil immersion objective introduces significant spherical aberration in an aqueous sample and the aberration is strongly depth dependent. A water immersion objective introduces less aberration of an infrared laser beam[26] and the aberration is nearly independent of imaging depth (until depths of ~200 μm).

Position detection can be performed either simply with a camera, or by using photodiode based techniques, the latter typically having the advantage of a higher space and time resolution and easier data processing. As depicted in Figure 1, a photodiode, either a quadrant photodiode detector (QPD) or a position sensitive detector (PSD) can be placed in the back focal plane of the objective. These photodiodes collect the forward scattered light and can easily achieve a spatial resolution down to a few nanometers in 3D[27] and a time resolution of μs.[28, 29] For certain purposes it is an advantage to employ a separate laser for position detection, which also allows for implementation of a feedback system with, e.g., acousto-optic[30] or electro-optic[31] deflectors.

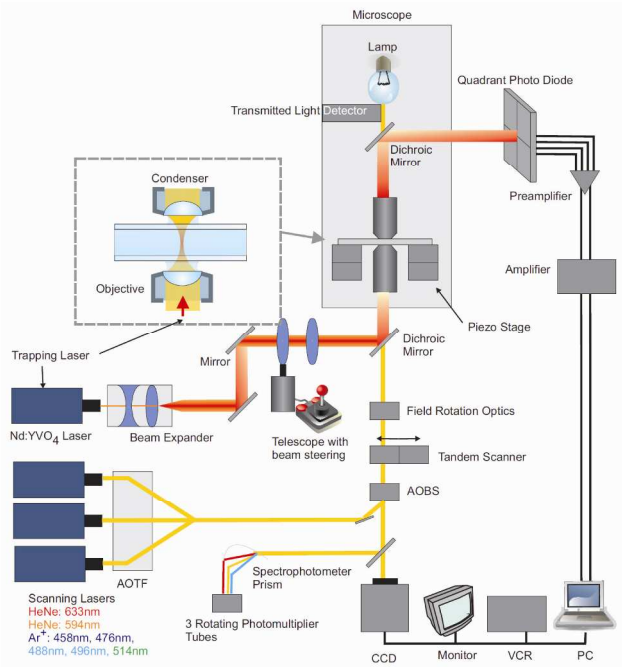

Figure 1. Illustration of an optical trap implemented in a confocal microscope. This equipment allows for simultaneous fluorescent visualization and force measurements and manipulation. Figure reproduced with permission from Richardson et al. [32]

Force calibration

In many experimental situations, the laser intensity in the trapping plane is not readily known and as precise calculations of optical forces are quite involved[33] and not necessarily available for complex geometries and handles, the force exerted by the trapping laser is most often found by calibration. A popular choice for precise and fast calibration relevant for *in vitro* experiments relies on recordings of the Brownian motion of an optically trapped dielectric bead. Such recordings are also denoted passive measurements because variations in the position of the trapped particle are caused by thermal fluctuations only and not by any active driving. In the simplest version of passive calibration, the bead radius and the viscosity of the surrounding liquid are assumed known. The trapping potential is assumed harmonic and by analysis of either the correlation function[34] or the power spectrum[35, 36] of the positions visited by the trapped bead, the passive calibration method returns a value for the spring constant κ of the trapping potential. With a value for κ at hand, a precise measurement of the position of a trapped object relative to its equilibrium position, x, will allow extraction of the force, $F = -\kappa x$.

In vivo the task of calibrating the optical trap becomes more complex. Now, the surrounding medium is no longer a liquid with known viscosity but may rather be modelled as a viscoelastic medium. If the trapped object is well characterized and available also outside the cell, one may determine its

trapping spring constant in a simple viscous liquid, e.g., through passive calibration. Then, the spring constant in the viscoelastic medium can be approximated by the spring constant found, but modified by accounting properly for the difference in refractive index between the two media. Another option is to use the limiting behavior at vanishing frequency of the real part of the viscoelastic modulus for the determination of the spring constant of the trap in the viscoelastic medium.[37] Often, however, the size and geometry of the object trapped within the living cell are unknown. In that case, two conceptually different approaches have been applied to determine the force exerted by the optical trap. One relies on the measurement of momentum changes imparted to the trapping laser light – and requires the ability to detect all the light scattered.[38, 39] A completely different approach relies on a combination of active and passive measurements.[40, 41] This approach allows for determination both of trap characteristics and of viscoelastic properties of the cytoplasm and does not require that the geometry or optical properties of the handle are known.[42] The procedure involves a series of experiments, as illustrated in Figure 2: In passive measurements (Fig. 2 a), time series of the positions visited by the trapped particle are recorded and power spectra, *P(f)*, are calculated. In active measurements (Fig. 2 b), while oscillating either the sample stage or the trapping laser, time series of the positions of the trapped bead are recorded and compared to the positions of the oscillating trap or stage, and a so-called relaxation spectrum is recorded.

In practice for the active measurements, the stage is oscillated at angular frequency ω, the stage position $x_S(t)$ is described as $x_S(t) = A_S \sin(\omega t + \varphi_S)$ and the motion of the trapped particle $x_P(t)$, recorded by a QPD, is fitted to the form $x_P(t) = A_P \sin(\omega t + \varphi_P)$. Subsequently, the data both from active and passive spectral measurements are combined to extract the information sought for, namely the spring constant of the trap, κ, and the viscoelastic modulus *G(f)*.

Figure 2. Illustration of the active-passive calibration method that is applicable in living systems. Sketch is not to scale. In part a), the passive part of the measurement protocol is illustrated. Recordings of the position of the trapped object inside the cell, here, a lipid granule inside a live *S. pombe* cell, allows for the experimenter to obtain a power spectrum, *P(f)*. In part b), the active part of

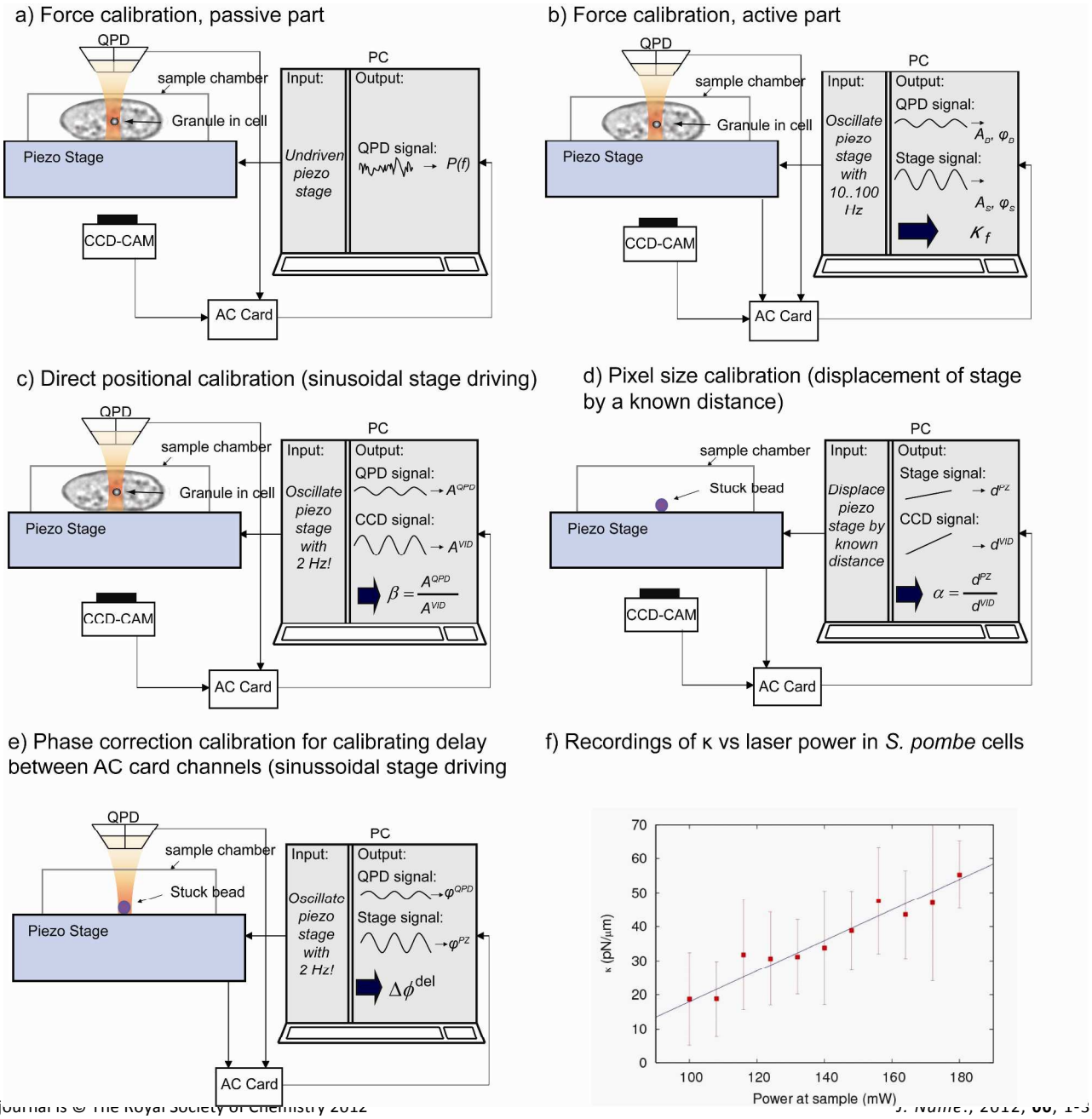

the protocol is illustrated, allowing to obtain values for the amplitude $A_{S/P}$ and phase $\varphi_{S/P}$ of both the stage (subscript *S*) that is actively driven, and the response of the trapped object (subscript *P*). In parts c)-e), experimental steps to determine parameters of the detection system are illustrated. In panel f), results obtained with trapped granules in a live *S. pombe* cell demonstrate that the spring constant of the trap, κ, increases linearly with the power of the trapping laser.

Intermediary steps (described by parts c)-e) in Fig. 2) ensure that the final outcome carries the correct physical dimensions. The active-passive method should be applied with a driving frequency chosen in frequency intervals that do not involve active processes, like action of molecular motors, as the method is based on the assumption that concepts of equilibrium thermodynamics are applicable. Fig. 2 f) demonstrates that the hallmarks of optical traps well-known from *in vitro* also apply *in vivo*: The spring constants characterizing optical trapping of lipid granules inside *S. pombe* yeast cells increase linearly with laser power.[42] This approach was also applied to investigate kinesin and dynein motors in live A549 human epithelial cells and in *Dictyostelium discoideum*.[43]

A slightly different, yet comparable method relies on fitting parameters of a proposed model for the viscoelasticity of the cytoplasm and has provided detailed information on microtubule motors in living cells, using endocytosed latex beads as tracer particles.[44]

What can be trapped?

Individual bio-molecules usually cannot be trapped because the induced dipole moment by the optical trap is not large enough. Therefore, a handle, that can be trapped, is typically specifically and firmly attached to the molecule of interest. Individual polystyrene and silica beads with diameters of several micrometers,[33, 45] quantum dots,[46] and various metallic nanoparticles with sizes down to ~ 10 nm can be optically trapped.[47, 48] For *in vivo* studies lipid granules that occur naturally inside most cells are particularly attractive as handles because they need not be internalized and can easily be optically trapped.[49-53] Furthermore, they are often transported by kinesin and dynein, hence, these motors are conveniently studied *in vivo* using lipid granules as handles. One shortcoming of optical tweezers is that they lack selectivity and therefore, all dielectric objects with an index of refraction that is larger than the surrounding medium and with an inducible dipole large enough will be trapped. *In vitro* such artefacts can be avoided or brought to a minimum by keeping the concentration of handles in the sample chamber very low. However, in living cell this is not possible and during the analysis one needs to take into account that maybe more handles are in the trap than aimed for.

Internalizing and conjugating the handle

Unless an endogenously occurring object, such as a lipid granule, is used as a handle for the optical manipulation, the handle needs to be internalized into the cell. Internalizing the handle may distort cellular integrity. The gentlest approach is probably to let the cell endocytose the handle. With many cell types this can be achieved simply by adding particles to the solution containing the cells. An example is given in Figure 3, which shows endocytosis of 60 nm gold nanoparticles by H727 neuroendocrine cancer cells. Conveniently, the size range of endocytotic uptake corresponds well to the size range of handles that can be stably optically trapped.[54] During endocytosis, nanoparticles in contact with the outer cell membrane, either non-specifically or by receptor recognition, are engulfed by large encapsulating lipid compartments called endosomes. Upon internalization, the endosomes are transported, typically along microtubules, to their designated location or the end terminal of the endosomal pathway, the lysosomes. The lysosomes are responsible for degrading the content of the endosomes by means of a highly hostile environment. If, however, one wishes to explore other parts of the cellular machinery than the endocytotic pathway, this approach has the shortcoming that the handle needs to be released from the coating vesicle and actively pulled to the location of interest inside the cell. Another pitfall is that during endocytosis, nanoparticles are typically encapsulated together as multiples (the diameter of the endosome is on the order of ~ 500 nm) and are therefore unavailable for individual manipulation unless efforts are made to release them from the endosomes.[54, 55]

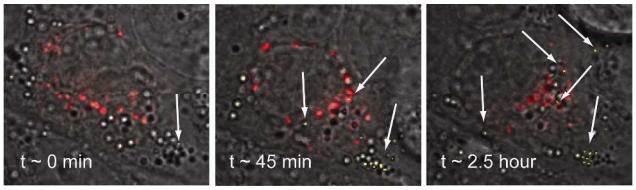

Fig 3: Endocytosis of 60 nm gold nanoparticles (yellow and marked by a white arrow) by H727 neuroendocrine cancer cells. The lysosomes (marked with Cell light lysosome-RFP; red) are the end destination of the endocytotic pathway and over time it is seen that the fraction of co-localization of the gold nanoparticles with the lysosomes increases.

Micropipette injection of particles is an invasive strategy for internalization. Here, the handles are injected into the cytoplasm or nucleus by penetrating the cell wall and membranes with a glass pipette typically with a diameter of 0.2 – 0.5 μm.[56] An example of this is shown in Figure 4 where a micropipette was used to perforate a H727 neuroendocrine cancer cell and deliver 125 nm gold nanoparticles into the cytoplasm. Another invasive internalization methodology is to optically inject gold nanoparticles into cells by tightly focussing a laser and burning a hole in the cell membrane (photoporation).[57] Electrophoretic shock has also been used as a delivery strategy, but that causes the cells to become severely stressed by the applied voltage.[58] The advantage of these more invasive approaches is that the handles can be mono-dispersedly internalized into the cell and in principle at any location inside the cell. These 'membrane rupturing approaches', however, have the drawback that they depend on the recovery of the cell membrane after penetration which might not always be possible. Alternative methodologies for internalizing nanoparticles in cells are reviewed in Refs. [58, 59]

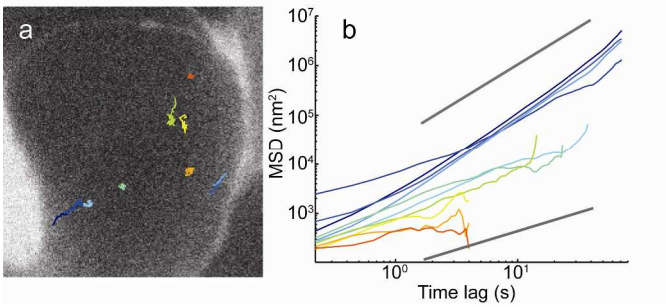

Figure 4: Diffusion of 125 nm gold nanoparticles that are micropipetted into a

neuroendocrine cancer cell. a) Image of a cell with the extra-cellular space fluorescently marked with Alexa Flour 488 hydrazide. Traces of diffusing gold nanoparticles are overlaid on the image. The traces are obtained from confocal scans (reflection mode). b) The mean squared displacements (MSD) of the micropipette injected gold nanoparticles, same colour code as in a). The lower full line has a slope of α=0.75, the upper a slope of α=1.5.

It is important that the handle is firmly and specifically attached to the molecule of interest in a one-to-one ratio. One of the main pitfalls of single molecule investigations, in particular *in vivo*, is that the handle, or visualization marker, may not be specifically attached to the molecule of interest or may be attached to multiple of those molecules. Ideally, handle attachment should be specific, strong and not affect the physiological state of the cell. Two successfully used schemes to specifically conjugate single molecules in the living cell are via receptor-ligand or antibody-antigen binding. The most commonly used conjugation is the biotin-streptavidin bond, whose strength is nearly the same as that of a covalent bond. Another, but weaker, antibody-antigen-based conjugation is the antidigoxigenin-digoxigenin bond. Other useful schemes include reactive cysteine residues and histidines. Many particles are commercially available with these functionalizations.

Though specific interactions between the biomolecule and the handle are important, reducing unspecific binding is also most crucial. Unspecific interactions between the handle and molecules in the media can easily introduce noise and artefacts. Proteins like bovine serum albumin and α-casein can significantly reduce unspecific interactions; however in the crowded cytoplasm inside the cell it is nearly impossible to prevent unspecific binding completely and clever control measurements must be done instead.

Heating

When performing optical tweezers measurements part of the focused laser light might be absorbed by the living cell or by the handle. Absorbed light is dissipated as heat into the surrounding tissue thus leading to a local temperature elevation. The absorption of infrared light by biological tissue or by silica and polystyrene handles is relatively minor and in aqueous environments typically leads to temperature elevations of 1^0C or less.[60] This value is consistent with a heating of ~1.15 C°/100 mW found in a cell confined by a 1064 nm trapping laser.[61]

The size range of which metallic nanoparticles can be stably trapped[48] makes them particularly favourable as force transducing handles inside the crowded cytoplasm. Furthermore, the size range is compatible with internalization through the endocytotic pathway. However, due to the plasmonic properties of metallic nanoparticles, they have significant absorption, also in the infrared, and can cause a substantial heating, depending on particle size,[62] shape,[63] and composition.[64] The temperature elevation at the surface of metallic nanoparticles can easily reach hundreds of degrees Celsius, however, if the particle is chosen small enough (e.g., with a diameter of 40 nm) and is irradiated at typical laser powers at the sample (~100 mW) the temperature elevation is too small to be detectable in a sensitive assay based upon the phase-dependent partitioning of fluorophores in a lipid bilayer,[62] that is, it is probably below a couple of degrees Celsius.

In conclusion, the temperature increase around optically trapped polystyrene beads, silica beads, or small metallic nanoparticles is probably so low that it would not interfere with physiological processes. Though, it should be noted that most temperature determining assays were carried out in an aqueous environment with larger heat conductivity than inside the cytoplasm; the temperature elevation inside a cell is expected to be larger than in an aqueous sample.

Physiological damage

Since Arthur Ashkin reported the survival of optically trapped microorganisms,[2] it has been a general consensus in the field that upon correct choice of laser wavelength and power, the physiological damage induced by optical traps is minor. Later studies have elaborated on this conjecture: One important effect of the infrared laser beam is that it produces free radicals and singlet oxygen, which has a high reactivity. Membranes and nucleic acids are sensitive to oxygen radicals that can cause oxidative stress and membrane rupture amongst others. Neuman et al.,[65] addressed the role of oxygen in photodamage in optical trapping of *E. coli* using laser wavelengths from 790 nm to 1064 nm. They measured the rotation rate of the flagella of a trapped *E. coli* under both aerobic and anaerobic conditions[65] and found that the photoinduced damage varied with laser wavelength and that it was significantly higher under aerobic than anaerobic conditions. An effect of photoinduced radicals was also observed in a single molecule assay tethering DNA between two microspheres under both aerobic and anaerobic conditions.[66] Generation of reactive oxygen species has been assessed for mammalian cell lines as well, where exposure to pulsed lasers was shown to be more likely to trigger the formation of reactive oxygen species than exposure to CW lasers.[67]

Trapping of microorganisms such as *E. coli* and *Listeria* has been shown to comprise the ability of the microorganism to maintain a proton gradient across the cell membrane.[68] The physiological damage was dependent on laser power and trapping time, hence, of the integrated power deposited in the organism. However, if trapping powers and exposure times were kept low, no physiological damage was observed.[68]

In conclusion, optical tweezers based on near infrared lasers do impose some degree of physiological damage and probably trigger stressful photochemical reactions.[53, 65, 69, 70] Therefore, for *in vivo* measurements, it is advisable to keep laser exposure time and power to a minimum.

Optical trapping inside the living cell

Objects that are large enough and with high enough optical contrast (mismatch in index of refraction) to the cytoplasm can be trapped inside the living cell. The trapped objects can be moved around in 3D and, thanks to the development of *in vivo* calibration techniques, the forces acting on the trapped objects can be measured. The biological processes in the cytoplasm are highly complex and many are regulated by mechanical forces, e.g., molecular motor and membrane protein motility, cell differentiation and cellular motility, as visualized in Figure 5.

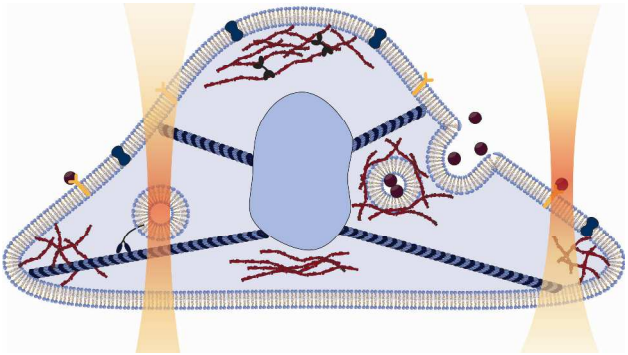

Figure 5. Illustration of the cellular machinery. Molecular motors such as kinesin and dynein carries cargo along microtubules (blue filaments), whereas the molecular motors in the myosin family move along actin (red filaments). The complex polymer network in the cytoplasm facilitates cellular transport and is also responsible for maintaining cell shape, organelle organization and for cell motility. The membrane contains a large variety of proteins responsible for signal transduction, cell adhesion and recognition, and transport of molecules and nutrients across the membrane. During endocytosis the membrane makes an invagination through which the object is engulfed. Anything with a large enough optical contrast to the cytoplasm can be optically trapped.

The local environment inside a cell may influence or temporarily modulate the function of biomolecule dynamics. Also, in contrast to most *in vitro* studies, a single motor cannot be isolated *in vivo* and many motors probably naturally work in a collective fashion in the living cell. In the subsequent sections we present the progress made using optical tweezers *in vivo*.

Microrheology

The first step towards measurements inside the living cell is to internalize and specifically attach the handle to the molecule of interest. As detailed above, there are several ways to do this. If the handles are micropipetted into the cell, some of these will diffuse randomly inside the cell and others will be picked up by molecular motors. An example of this is shown in Figure 4, where Fig. 4a) shows an image of H727 neuroendocrine cancer cells. Gold nanoparticles were microinjected into the cell and the traces of the injected particles tracked. Some of the particles hardly moved (red traces), others performed subdiffusive motion (yellow and light blue traces) while others moved in a linear fashion (blue traces). Dynamics within the cytoplasm can be described by different classes of diffusion. These are characterized by the scaling behaviour of the mean squared displacement, $\mathrm{MSD}(\tau) = \langle [r(t+\tau) - r(t)]^2 \rangle$, $r(t)$ being the position of the particle at time t and τ being the time lag. $\mathrm{MSD}=2Dt^{\alpha}$, where D is the diffusion constant and α is the scaling exponent. The scaling exponent, α, yields information on whether the motion is subdiffusive ($\alpha < 1$), normal diffusion ($\alpha = 1$), or superdiffusive ($\alpha > 1$). In the experiment depicted in Fig. 4, the red traces have $\alpha \sim 0$, thus exhibiting confined diffusion, the yellow and light blue traces have $\alpha \sim 0.75$, hence, are subdiffusive, as often observed for passive tracers inside living cells,[42, 51, 71, 72] in accordance with the behavior of semiflexible polymer networks.[73] The blue traces are the result of superdiffusion ($\alpha \sim 1.5$) in accordance with observations of 1-2 µm polystyrene beads in a study of human SV80 cells[74] and micro-injected quantum dots in HeLa cells.[75] If the goal is to study molecular motors inside a living cell, then the super-diffusive particles are the tracers most likely to be bound to active molecular motors.

Optical tweezers have successfully been used to expand microrheology measurements in living cells. The timescales probed with optical tweezers are on the order of (10^{-6} – 10^{-3} s),[42, 51, 71] a regime that is unavailable to standard video based rheology measurements (> 0.01 s), [42, 51] thus making optical tweezers able to access regimes where interesting dynamics, e.g., weak ergodicity breaking occurs.[52]

Also the impact of the cytoskeletal subcomponents on cellular microrhelogy has been explored. It was found that passive tracers, lipid granules inside *S. pombe*, performed subdiffusional motion at all times during the cell cycle, albeit with a significantly larger scaling exponent during mitosis ($\alpha \sim 0.84$) than during interphase ($\alpha \sim 0.81$).[71] This was attributed to the fact that the network of microtubules are denser, thus making the cytoplasm more elastic during mitosis.[71] Similar lipid granules were also shown to diffuse more freely upon disruption of cellular actin.[51]

The contribution of intermediate filaments to the viscoelasticity of the cytoplasm has recently been assessed using mouse embryonic fibroblasts.[76] Here the influence of vimentin, one of the most common intermediate filaments, was studied using both optical tweezers and video-based particle tracking. The motion of endogenous granules was found to decrease in the presence of vimentin intermediate filaments suggesting that the vimentin network helps localizing cytoplasmic organelles by stiffening the local environment.

As described above, also the viscoelastic modulus $G(f)$ can be extracted from passive and active *in vivo* optical tweezers calibration. This was done using optically trapped granules inside an *S. pombe* cell and showed that the elastic response of the viscoelastic modulus Re[G], also denoted G', increased with an exponent of $\alpha = 0.75$ as a function of frequency,[42] consistent with earlier data.[51] In the narrow frequency window between 5 and 75 Hz G' for *S. pombe* was found to range from $G' \sim 4$ to 30 Pa.[42, 51] In mouse embryonic fibroblasts with an intact vimentin network, the elastic response of the viscoelastic modulus was found to be $G' \sim 10$ Pa at 1 Hz with a diffusion exponent of $\alpha = 0.25$ in the frequency range from 1 to 100 Hz.[76] This viscoelastic modulus is significantly larger than the value obtained in *S. pombe* at 1 Hz ($G' \sim 1$ Pa),[42, 51] however when assessed by the diffusion exponent the cytoplasm of the mouse embryonic fibroblasts is also significantly more elastic ($\alpha = 0.25$)[76] than the cytoplasm of *S. pombe* ($\alpha \sim 0.75$).[42, 51] Further, when comparing G' from wild-type mouse embryonic fibroblasts at 1 Hz ($G' \sim 10$ Pa) to G' from vimentin deficient mouse embryonic fibroblasts cells at the same frequency ($G' \sim 5$ Pa) it is clear that the presence of vimentin intermediate filaments stiffens the cytoplasm.[76]

Membrane protein dynamics

The plasma membrane of a cell consists of a phospholipid bilayer that is compartmentalized into many small domains. Embedded into the membrane is a large variety of proteins having essential roles for proper cell function, for instance for communication between the exterior and interior of the cell, transportation across the membrane of ions, nutrients and enzymes, and cell adhesion and recognition.

One of the early applications of optical tweezers *in vivo* was to characterize diffusion of proteins in the membrane of eukaryotic cells.[77, 78] Handles composed of 210 nm latex beads or 40 nm colloidal gold particles were in one study attached to a membrane protein and dragged laterally through the plasma membrane of normal rat kidney fibroblastic cells.[78] The force required to drag the protein ranged from 0.05 pN to 0.8 pN, the large range probably signifying the viscoelastic heterogeneity

of the plasma membrane which is also known to be compartmentalized. In a later study, a method was developed by which the diffusion of the protein in its native location (without dragging it large distances through the membrane) was studied by optical tweezers.[79] In this study GPI-anchored proteins appeared to localize at a lipid raft for extended periods of time.[79]

Optical tweezers were also used to study the diffusion of proteins in the membrane of prokaryotes. Gram-negative bacteria have several membrane layers in contrast to that of most mammalian cells. In addition to the inner bilayer Gram-negative bacteria also have both an outer membrane consisting of a lipopolysaccharide coat and a peptidoglycan layer separating the plasma membrane from the outer membrane. Using optical tweezers, the local diffusion of a single transmembrane protein, the λ-receptor, in the outer membrane of an *E. coli* was probed by measuring its Brownian motion.[80] It was found that the λ-receptor had a low diffusion constant compared to diffusion in the eukaryotic membranes. Also, the dynamics of the λ-receptor was found to be energy dependent[81] and to correlate with the dynamic reassembly of the peptidoglycan layer.[82] These findings indicated that the λ-receptor is attached to the peptidoglycan layer and that its diffusion is closely linked to the metabolism of the cell, hence, it is not a pure thermal diffusion. These results suggests that membrane diffusion studied *in vitro* will be different from *in vivo* studies as the active component linked to cell metabolism is lacking *in vitro*.

Molecular motors

Large molecules, filaments or organelles in the living cell are transported, translocated or rotated actively by motor proteins. These motor proteins use ATP to generate force as they perform their biased motions.

Two classes of motors that transport cargo along microtubules have been identified: the kinesin family that translocates towards the microtubules plus-end and cytoplasmic dynein translocating towards the minus-end. *In vivo* investigations have shown that molecular motors perform saltatory motion in the cellular viscoelastic environment[83, 84] and that the stall force, i.e., the minimum force needed to stall a motor pulling on its cargo, for kinesin family is 5-7 pN[43] and for dynein is 1-8 pN.[22, 43, 44]

The consensus is that *in vivo* several motors are typically involved in cargo transport[85] and, in particular, that cargo is transported along microtubules by complements of kinesin and dynein motors[86]. Furthermore, in a study using endogenously occurring lipid granules as handles in an A549 human cancer cell, the forces exerted by individual motors are found to be additive.[49] Thus, the stall force of *in vivo* active transport allows the identification of the individual motors in the complement.

From a study of phagocytosed latex beads in mouse macrophage cells, the cargo motility along microtubules was found to be the result of a collective motion of a few kinesin molecules moving towards the plus-end, and many dynein moving towards the minus-end.[44] It was also shown that coupled motors at high loads often synchronize their steps to move in the characteristic 8 nm steps along microtubules.[44] Furthermore, in an assay with kinesin-1 and dynein-driven lipid droplets in *Drosophila* embryos, it was found that if the cargo transported in one direction was stalled and detached, it was more prone to be transported in the same direction when resumed.[87]

The stall forces of kinesin and dynein *in vivo* were investigated using endogenous lipid granules in A549 human cancer cells and latex beads in *Dictyostelium discoideum* as optical trapping handles.[43] Stall forces, depicted in Fig. 6 a) and b) for A549 cells and in Fig. 6 c) and d) for *Dictyostelium*, were shown to be different in the plus-end and minus-end directions. Interestingly, the plus-end directed (outward) stall force was found to be lower than the *in vitro* value for kinesin, implying that often both kinesins and dyneins attach to the cargo and pull in opposite directions in a tug-of-war manner.[88-90] In the minus-end direction (inwards) the stalling forces were higher than measured for individual dynein *in vitro*, implying that several dynein (and no kinesins) were acting in collective fashion during inwards motion. Fig. 6 e) shows examples of the dislocation of the cargo, the time traces show regions of linear movement in both directions interrupted by stalls.

It has been proposed that even though both dynein and kinesin are bound to the cargo, only motors of one polarity are active at any instant of time, with the activity being reversible by aid of a co-factor.[22] A candidate co-factor has been identified in a study of kinesin in monkey fibroblast, where casein kinase 2 is found to regulate kinesins that are attached to their cargo.[91] Also, dyneins are found to team up to generate large forces.[92]

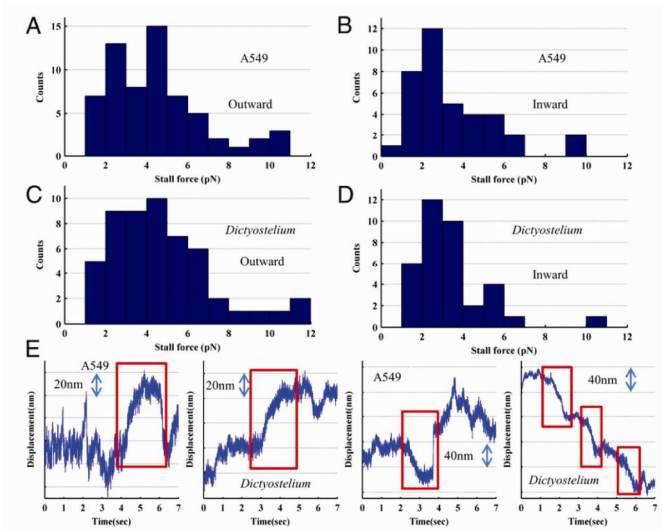

Fig. 6: *In vivo* stall force measurements for lipid granules in A549 human cancer A549 (A-B) and for endocytosed latex beads in *Dictyostelium* (C-D). **A-B:** Stall force histograms of outward (A) and inward cargo motility (B) in A549 cells. **C-D:** Stall force histograms of outward (C) and inward cargo motility (D in *Dictyostelium*). The distributions for the two cell types are very similar. Both imply significant differences between the stall forces for inward and outward motion. **E:** Examples of cargo traces showing periods of active motion in both directions interrupted by stalls. Reproduced with permission from Blehm et al. [43].

Filapodia dynamics has been shown via optical tweezers to be regulated partly by F-actin filament polymerization and depolymerisation,[93] and partly by mechanical work conducted by actin-based myosin molecular motors, inducing a retrograde flow.[94] Using optically trapped IgG-coated polystyrene beads attached to the tip of a filopodium discrete steps during filapodia retraction were observed, the step sizes were ~36 nm, consistent with myosin being the motor responsible for filapodia retraction.[94] As forces up to 19 pN were measured, most likely several molecular myosin motors work cooperatively to retract filapodia.

The status of the field is that the motors most frequently studied with optical tweezers are kinesin and dynein. Without doubt, this is attributed to the fact that these motors carry endogenously occurring lipid granules that are easily optically trapped and serve as excellent force-transducing handles. However, there are also other endogenously occurring 'objects' in the cell that can be optically manipulated. One such example is the chromosomes that can be trapped to estimate the forces exerted by molecular motors onto the mitotic spindle, in this manner the stalling force for chromosome movements in *Mesostoma* spermatocytes was estimated to be 2.3 pN and in crane-fly spermatocytes to be 6-10 pN.[95]

Outlook

Until now optical tweezers have predominantly been used in vitro, however, as most of the challenges connected to *in vivo* use of this technique[24] have now been overcome, exciting novel quantitative *in vivo* single molecule results are now beginning to appear[5, 86]. Though optical tweezers have themselves very large potential for single molecule *in vivo* investigations, another advantage is that they can easily be combined with other techniques, such as fluorescent imaging,[96] which gives an even larger potential for revealing connections between, e.g., mechanical force and biochemical regulation. Recently, a clever methodology was invented where super-resolution STED microscopy was combined with optical trapping; this equipment was used to reveal protein dynamics on DNA.[97] This type of super-resolution microscopy combined with state-of-the-art force measuring optical traps has huge potential for uncovering fundamental mechanical-biochemical action-reaction schemes inside the living cell.

So far, all reported *in vivo* single molecule optical tweezers investigations were carried out in 2D cell cultures, on single celled microorganisms, or with single cells isolated from multi-cell organisms or tissue. However, as laser light has the ability to penetrate deep into biological tissue, it is likely that optical traps could be used to investigate also the mechanics within multi-cellular organisms or tissue. Or, as optical tweezers have proven able to trap synaptic vesicles,[98] maybe the technique can even shed light on the fundamental mechanism and mechanics governing nerve conduction and development of neuronal diseases.

Acknowledgements

We acknowledge financial support from the Carlsberg Foundation and an excellence grant from the University of Copenhagen.

Notes and references

[a] Niels Bohr Institute, University of Copenhagen, Copenhagen, Denmark.
[b] Department of Physics, Technical University of Denmark, Denmark.

1. A. Ashkin, K. Schutze, J. M. Dziedzic, U. Euteneuer and M. Schliwa, *Nature*, 1990, **348**, 346-348.
2. A. Ashkin and J. M. Dziedzic, *Science*, 1987, **235**, 1517-1520.
3. K. C. Neuman and A. Nagy, *Nature methods*, 2008, **5**, 491-505.
4. C. Veigel and C. F. Schmidt, *Nature reviews. Molecular cell biology*, 2011, **12**, 163-176.
5. L. B. Oddershede, *Nature chemical biology*, 2012, **8**, 879-886.
6. M. J. Rust, M. Bates and X. Zhuang, *Nature methods*, 2006, **3**, 793-795.
7. T. A. Klar, S. Jakobs, M. Dyba, A. Egner and S. W. Hell, *Proceedings of the National Academy of Sciences of the United States of America*, 2000, **97**, 8206-8210.
8. D. T. Tambe, C. C. Hardin, T. E. Angelini, K. Rajendran, C. Y. Park, X. Serra-Picamal, E. H. Zhou, M. H. Zaman, J. P. Butler, D. A. Weitz, J. J. Fredberg and X. Trepat, *Nature materials*, 2011, **10**, 469-475.
9. R. D. Gonzalez-Cruz, V. C. Fonseca and E. M. Darling, *Proceedings of the National Academy of Sciences of the United States of America*, 2012, **109**, E1523-1529.
10. K. Svoboda, C. F. Schmidt, B. J. Schnapp and S. M. Block, *Nature*, 1993, **365**, 721-727.
11. K. Visscher, M. J. Schnitzer and S. M. Block, *Nature*, 1999, **400**, 184-189.
12. C. L. Asbury, A. N. Fehr and S. M. Block, *Science*, 2003, **302**, 2130-2134.
13. C. Veigel, L. M. Coluccio, J. D. Jontes, J. C. Sparrow, R. A. Milligan and J. E. Molloy, *Nature*, 1999, **398**, 530-533.
14. C. Veigel, J. E. Molloy, S. Schmitz and J. Kendrick-Jones, *Nature cell biology*, 2003, **5**, 980-986.
15. L. Laan, J. Husson, E. L. Munteanu, J. W. Kerssemakers and M. Dogterom, *Proceedings of the National Academy of Sciences of the United States of America*, 2008, **105**, 8920-8925.
16. M. J. Footer, J. W. Kerssemakers, J. A. Theriot and M. Dogterom, *Proceedings of the National Academy of Sciences of the United States of America*, 2007, **104**, 2181-2186.
17. M. D. Wang, H. Yin, R. Landick, J. Gelles and S. M. Block, *Biophysical journal*, 1997, **72**, 1335-1346.
18. P. Gross, N. Laurens, L. B. Oddershede, U. Bockelmann, E. J. G. Peterman and G. J. L. Wuite, *Nat Phys*, 2011, **7**, 731-736.
19. L. Shokri, B. Marintcheva, M. Eldib, A. Hanke, I. Rouzina and M. C. Williams, *Nucleic Acids Res*, 2008, **36**, 5668-5677.
20. J. van Mameren, P. Gross, G. Farge, P. Hooijman, M. Modesti, M. Falkenberg, G. J. Wuite and E. J. Peterman, *Proceedings of the National Academy of Sciences of the United States of America*, 2009, **106**, 18231-18236.
21. T. Paramanathan, I. Vladescu, M. J. McCauley, I. Rouzina and M. C. Williams, *Nucleic Acids Res*, 2012, **40**, 4925-4932.
22. S. P. Gross, M. A. Welte, S. M. Block and E. F. Wieschaus, *The Journal of cell biology*, 2000, **148**, 945-956.
23. Z. Wang, S. Khan and M. P. Sheetz, *Biophysical journal*, 1995, **69**, 2011-2023.
24. Y. F. Dufrene, E. Evans, A. Engel, J. Helenius, H. E. Gaub and D. J. Muller, *Nature methods*, 2011, **8**, 123-127.
25. A. Kyrsting, P. M. Bendix and L. B. Oddershede, *Nano letters*, 2013, **13**, 31-35.
26. S. N. S. Reihani, S. A. Mir, A. C. Richardson and L. B. Oddershede, *Journal of Optics*, 2011, **13**.
27. A. Rohrbach and E. H. K. Stelzer, *J Appl Phys*, 2002, **91**, 5474-5488.
28. K. C. Neuman and S. M. Block, *The Review of scientific instruments*, 2004, **75**, 2787-2809.
29. F. Gittes and C. F. Schmidt, *Optics letters*, 1998, **23**, 7-9.
30. K. Visscher and S. M. Block, *Methods in enzymology*, 1998, **298**, 460-489.
31. M. T. Valentine, N. R. Guydosh, B. Gutierrez-Medina, A. N. Fehr, J. O. Andreasson and S. M. Block, *Optics letters*, 2008, **33**, 599-601.
32. A. C. Richardson, N. Reihani and L. B. Oddershede, *Proceedings of SPIE*, 2006, **6326**, 632628-(1-10).
33. A. Rohrbach, *Physical review letters*, 2005, **95,** 168102-(1-4).
34. A. Pralle, E. L. Florin, E. H. K. Stelzer and J. K. H. Horber, *Appl Phys a-Mater*, 1998, **66**, S71-S73.
35. F. Gittes and C. F. Schmidt, *Method Cell Biol*, 1998, **55**, 129-156.
36. K. Berg-Sørensen and H. Flyvbjerg, *Review of Scientific Instruments*, 2004, **75**, 594-612.
37. M. Atakhorrami, J. I. Sulkowska, K. M. Addas, G. H. Koenderink, J. X. Tang, A. J. Levine, F. C. MacKintosh and C. F. Schmidt, *Phys Rev E*, 2006, **73**.
38. A. Farre and M. Montes-Usategui, *Optics express*, 2010, **18**, 11955-11968.
39. S. B. Smith, Y. Cui and C. Bustamante, *Methods in enzymology*, 2003, **361**, 134-162.

40. M. Fischer and K. Berg-Sørensen, *Journal of Optics A: Pure and Applied Optics*, 2007, **9**, S239.
41. M. Fischer, A. C. Richardson, S. N. Reihani, L. B. Oddershede and K. Berg-Sorensen, *The Review of scientific instruments*, 2010, **81**, 015103.
42. J. Mas, A. C. Richardson, S. N. S. Reihani, L. B. Oddershede and K. Berg-Sørensen, *Physical Biology*, 2013, **10**, 046006.
43. B. H. Blehm, T. A. Schroer, K. M. Trybus, Y. R. Chemla and P. R. Selvin, *Proceedings of the National Academy of Sciences of the United States of America*, 2013, **110**, 3381-3386.
44. A. G. Hendricks, E. L. Holzbaur and Y. E. Goldman, *Proceedings of the National Academy of Sciences of the United States of America*, 2012, **109**, 18447-18452.
45. J. R. Moffitt, Y. R. Chemla, S. B. Smith and C. Bustamante, *Annu Rev Biochem*, 2008, **77**, 205-228.
46. L. Jauffred, A. C. Richardson and L. B. Oddershede, *Nano letters*, 2008, **8**, 3376-3380.
47. P. M. Hansen, V. K. Bhatia, N. Harrit and L. Oddershede, *Nano letters*, 2005, **5**, 1937-1942.
48. P. M. Bendix, L. Jauffred, K. Norregaard and L. B. Oddershede, *Selected Topics in Quantum Electronics, IEEE Journal of*, 2014, **20**, 1-12.
49. P. A. Sims and X. S. Xie, *Chemphyschem : a European journal of chemical physics and physical chemistry*, 2009, **10**, 1511-1516.
50. G. T. Shubeita, S. L. Tran, J. Xu, M. Vershinin, S. Cermelli, S. L. Cotton, M. A. Welte and S. P. Gross, *Cell*, 2008, **135**, 1098-1107.
51. I. M. Tolic-Norrelykke, E. L. Munteanu, G. Thon, L. Oddershede and K. Berg-Sorensen, *Physical review letters*, 2004, **93**, 078102.
52. J. H. Jeon, V. Tejedor, S. Burov, E. Barkai, C. Selhuber-Unkel, K. Berg-Sorensen, L. Oddershede and R. Metzler, *Physical review letters*, 2011, **106**, 048103.
53. L. Sacconi, I. M. Tolic-Norrelykke, C. Stringari, R. Antolini and F. S. Pavone, *Applied optics*, 2005, **44**, 2001-2007.
54. T.-G. Iversen, T. Skotland and K. Sandvig, *Nano Today*, 2011, **6**, 176-185.
55. S. H. Wang, C. W. Lee, A. Chiou and P. K. Wei, *Journal of nanobiotechnology*, 2010, **8**, 33.
56. Y. Zhang and L.-C. Yu, *BioEssays*, 2008, **30**, 606-610.
57. C. McDougall, D. J. Stevenson, C. T. A. Brown, F. Gunn-Moore and K. Dholakia, *Journal of Biophotonics*, 2009, **2**, 736-743.
58. J. B. Delehanty, H. Mattoussi and I. L. Medintz, *Analytical and bioanalytical chemistry*, 2009, **393**, 1091-1105.
59. R. Levy, U. Shaheen, Y. Cesbron and V. See, *Nano reviews*, 2010, **1**.
60. E. J. Peterman, F. Gittes and C. F. Schmidt, *Biophysical journal*, 2003, **84**, 1308-1316.
61. Y. Liu, D. K. Cheng, G. J. Sonek, M. W. Berns, C. F. Chapman and B. J. Tromberg, *Biophysical journal*, 1995, **68**, 2137-2144.
62. P. M. Bendix, S. N. Reihani and L. B. Oddershede, *ACS nano*, 2010, **4**, 2256-2262.
63. H. Y. Ma, P. M. Bendix and L. B. Oddershede, *Nano letters*, 2012, **12**, 3954-3960.
64. H. Ma, P. Tian, J. Pello, P. M. Bendix and L. B. Oddershede, *Nano letters*, 2014.
65. K. C. Neuman, E. H. Chadd, G. F. Liou, K. Bergman and S. M. Block, *Biophysical journal*, 1999, **77**, 2856-2863.
66. M. P. Landry, P. M. McCall, Z. Qi and Y. R. Chemla, *Biophysical journal*, 2009, **97**, 2128-2136.
67. S. K. Mohanty, M. Sharma and P. K. Gupta, *Photochemical & photobiological sciences : Official journal of the European Photochemistry Association and the European Society for Photobiology*, 2006, **5**, 134-139.
68. M. B. Rasmussen, L. B. Oddershede and H. Siegumfeldt, *Applied and environmental microbiology*, 2008, **74**, 2441-2446.
69. H. Liang, K. T. Vu, P. Krishnan, T. C. Trang, D. Shin, S. Kimel and M. W. Berns, *Biophysical journal*, 1996, **70**, 1529-1533.
70. G. Leitz, E. Fallman, S. Tuck and O. Axner, *Biophysical journal*, 2002, **82**, 2224-2231.
71. C. Selhuber-Unkel, P. Yde, K. Berg-Sorensen and L. B. Oddershede, *Phys Biol*, 2009, **6**, 025015.
72. S. Yamada, D. Wirtz and S. C. Kuo, *Biophysical journal*, 2000, **78**, 1736-1747.
73. F. Gittes and F. C. MacKintosh, *Phys Rev E*, 1998, **58**, R1241-R1244.
74. A. Caspi, R. Granek and M. Elbaum, *Physical review. E, Statistical, nonlinear, and soft matter physics*, 2002, **66**, 011916.
75. S. Courty, C. Luccardini, Y. Bellaiche, G. Cappello and M. Dahan, *Nano letters*, 2006, **6**, 1491-1495.
76. M. Guo, A. J. Ehrlicher, S. Mahammad, H. Fabich, M. H. Jensen, J. R. Moore, J. J. Fredberg, R. D. Goldman and D. A. Weitz, *Biophysical journal*, 2013, **105**, 1562-1568.
77. M. Edidin, S. C. Kuo and M. P. Sheetz, *Science*, 1991, **254**, 1379-1382.
78. Y. Sako and A. Kusumi, *The Journal of cell biology*, 1995, **129**, 1559-1574.
79. A. Pralle, P. Keller, E. L. Florin, K. Simons and J. K. Horber, *The Journal of cell biology*, 2000, **148**, 997-1008.
80. L. Oddershede, J. K. Dreyer, S. Grego, S. Brown and K. Berg-Sorensen, *Biophysical journal*, 2002, **83**, 3152-3161.
81. T. Winther, L. Xu, K. Berg-Sorensen, S. Brown and L. B. Oddershede, *Biophysical journal*, 2009, **97**, 1305-1312.
82. T. Winther and L. B. Oddershede, *Current pharmaceutical biotechnology*, 2009, **10**, 486-493.
83. M. A. Welte, S. P. Gross, M. Postner, S. M. Block and E. F. Wieschaus, *Cell*, 1998, **92**, 547-557.
84. A. L. Jolly, H. Kim, D. Srinivasan, M. Lakonishok, A. G. Larson and V. I. Gelfand, *Proceedings of the National Academy of Sciences of the United States of America*, 2010, **107**, 12151-12156.
85. S. P. Gross, M. Vershinin and G. T. Shubeita, *Current biology : CB*, 2007, **17**, R478-486.
86. B. H. a. S. Blehm, P.R., *Chemical Reviews*, 2014.
87. C. Leidel, R. A. Longoria, F. M. Gutierrez and G. T. Shubeita, *Biophysical journal*, 2012, **103**, 492-500.
88. V. Soppina, A. K. Rai, A. J. Ramaiya, P. Barak and R. Mallik, *Proceedings of the National Academy of Sciences of the United States of America*, 2009, **106**, 19381-19386.
89. A. G. Hendricks, E. Perlson, J. L. Ross, H. W. Schroeder, M. Tokito and E. L. F. Holzbaur, *Current biology : CB*, 2010, **20**, 697-702.
90. A. Kunwar, S. K. Tripathy, J. Xu, M. K. Mattson, P. Anand, R. Sigua, M. Vershinin, R. J. McKenney, C. C. Yu, A. Mogilner and S. P. Gross, *Proceedings of the National Academy of Sciences of the United States of America*, 2011, **108**, 18960-18965.
91. J. Xu, B. J. Reddy, P. Anand, Z. Shu, S. Cermelli, M. K. Mattson, S. K. Tripathy, M. T. Hoss, N. S. James, S. J. King, L. Huang, L. Bardwell and S. P. Gross, *Nature communications*, 2012, **3**, 754.
92. Arpan K. Rai, A. Rai, Avin J. Ramaiya, R. Jha and R. Mallik, *Cell*, 2013, **152**, 172-182.
93. T. Bornschlogl, S. Romero, C. L. Vestergaard, J. F. Joanny, G. T. V. Nhieu and P. Bassereau, *Proceedings of the National Academy of Sciences of the United States of America*, 2013, **110**, 18928-18933.
94. H. Kress, E. H. Stelzer, D. Holzer, F. Buss, G. Griffiths and A. Rohrbach, *Proc Natl Acad Sci U S A*, 2007, **104**, 11633-11638.
95. J. Ferraro-Gideon, R. Sheykhani, Q. Y. Zhu, M. L. Duquette, M. W. Berns and A. Forer, *Mol Biol Cell*, 2013, **24**, 1375-1386.
96. M. J. Lang, P. M. Fordyce, A. M. Engh, K. C. Neuman and S. M. Block, *Nature methods*, 2004, **1**, 133-139.
97. I. Heller, G. Sitters, O. D. Broekmans, G. Farge, C. Menges, W. Wende, S. W. Hell, E. J. G. Peterman and G. J. L. Wuite, *Nature methods*, 2013, **10**, 910-U132.
98. P. M. Bendix and L. Oddershede, *Biophysical journal*, 2012, **102**, 87a-87a.

Kamilla Nørregaard received her B.S. degree in physics in 2009 and the Cand. Scient degree in physics in 2011 at the University of Copenhagen. Currently she is working on her Ph.D. in biophysics under the guidance of Poul M. Bendix and Lene B. Oddershede. Her research interests include

plasmonic heating and trapping of nanoparticles, nanoparticle mediated photothermal cancer therapy, and nanoparticle delivered gene therapy.

Liselotte Jauffred received her B.S. degree in mathematics and physics in 2004 and the Cand.Scient. degree in physics in 2006 at the University of Copenhagen. She graduated as a Ph.D. from the Niels Bohr Institute (NBI) within biophysics in 2010. As a postdoc she has worked at the FOM Institute AMOLF in Amsterdam and is currently postdoc at NBI. Her research includes interactions between light and quantum dots and she was the first to visualize and quantitate the forces exerted on an optically trapped quantum dot.

Kirstine Berg-Sørensen, received the Cand. Scient. degree in chemistry and physics from University of Aarhus (AU) in 1991 and the Ph.D. degree in physics from AU in 1994. She visited the Laboratoire Kastler-Brossel, École Normale Superieure, Paris 1992 and was a postdoc at Rowland Institute for Science, Cambridge MA 1994-1995. In 1998 she established the optical tweezers group at the NBI with funding from the Danish Research Councils. Since 2005, she has been associate professor at the Dept of Physics, Technical University of Denmark. In her early research years, she investigated optical trapping and condensation of cold atomic gases whereas more recent research interests involve data analysis in connection with optical manipulation in biological specimen and experiments to do so. In addition, she investigates flow in model systems for plants.

Lene B. Oddershede, PI of the optical tweezers group at the Niels Bohr Institute (NBI), received the Cand. Scient degree in mathematics and physics from University of Southern Denmark (SDU) in 1995 and the PhD degree in physics from SDU in 1998. She visited the James Frank Institute, University of Chicago 1996-1997. In 1998 she became an assistent Professor and constructed the optical tweezers laboratory at NBI, University of Copenhagen. In 2003 she was tenured as an associate professor at the NBI. In 2003 she received the Young Investigator Award from the Danish Optical Society and in 2011 the Silver Medal from the Danish Royal Academy of Sciences. Her research interests include the biophotonical and nanotoxological properties of nanoparticles and their potential use in biological contexts. Also, she is interested in optical manipulation of biological specimen.